



Cite this: *Nanoscale*, 2019, **11**, 16284

Received 31st May 2019,
Accepted 25th July 2019

DOI: 10.1039/c9nr04653d

rsc.li/nanoscale

Proteoliposomes as energy transferring nanomaterials: enhancing the spectral range of light-harvesting proteins using lipid-linked chromophores†

Ashley M. Hancock,^{id a,b} Sophie A. Meredith,^{id a,b} Simon D. Connell,^{id a,b}
Lars J. C. Jeuken^{id b,c} and Peter G. Adams^{id *a,b}

Bio-hybrid nanomaterials have great potential for combining the most desirable aspects of biomolecules and the contemporary concepts of nanotechnology to create highly efficient light-harvesting materials. Light-harvesting proteins are optimized to absorb and transfer solar energy with remarkable efficiency but have a spectral range that is limited by their natural pigment complement. Herein, we present the development of model membranes (“proteoliposomes”) in which the absorption range of the membrane protein Light-Harvesting Complex II (LHCII) is effectively enhanced by the addition of lipid-tethered Texas Red (TR) chromophores. Energy transfer from TR to LHCII is observed with up to 94% efficiency and increased LHCII fluorescence of up to three-fold when excited in the region of lowest natural absorption. The new self-assembly procedure offers the modularity to control the concentrations incorporated of TR and LHCII, allowing energy transfer and fluorescence to be tuned. Fluorescence Lifetime Imaging Microscopy provides single-proteoliposome-level quantification of energy transfer efficiency and confirms that functionality is retained on surfaces. Designer proteoliposomes could act as a controllable light-harvesting nanomaterial and are a promising step in the development of bio-hybrid light-harvesting systems.

Introduction

Biological systems are a source of inspiration in solar energy and nanotechnology research,^{1–6} because the early stages of energy absorption and transfer in photosynthesis have an

efficiency approaching unity.⁷ The membrane proteins which undertake photosynthetic light-harvesting (LH) act in a conceptually similar way to a satellite dish, whereby antenna proteins channel energy towards Reaction Centre proteins which perform photochemistry.⁸ LH membrane proteins have a 3-D polypeptide structure which acts as a scaffold to precisely arrange chromophores at high density in such a manner that energy absorption and transfer are extremely efficient.⁹ Light-harvesting complex II (LHCII)¹⁰ acts as the primary antenna protein for plants and is estimated to be the most abundant membrane protein on Earth due to its high density in the membranes of chloroplasts. LHCII has a heterotrimeric structure with each monomer containing fourteen chlorophyll and four carotenoids;¹⁰ this combination of chromophores gives the protein complex a high absorption coverage across the visible spectrum aside from the ‘green gap’ of minimal absorption between 520–620 nm. Several studies have filled this green gap with complementary chromophores which absorb strongly in this spectral region and transfer energy to the protein *via* Förster Resonance Energy Transfer (FRET). This was first demonstrated by covalently attaching chromophores to LH membrane proteins isolated in detergents, the chosen chromophores including synthetic organic compounds^{11–14} and quantum dots.^{15,16} FRET has also been demonstrated between non-covalently coupled chromophores incorporated into lipid bilayers^{17–19} or polymer micelles.^{20–22} LHCII has previously been integrated into model membranes, *e.g.*, lipid vesicles^{23–28} or lipid nanodiscs,^{28,29} and these have been studied to understand its biophysical properties, but have not yet been exploited to enhance its spectral range. Adding the chromophore to the lipid membrane would have several advantages compared to covalent modification of LH proteins: (i) lipids provide a more native environment for membrane proteins than detergent, (ii) membranes readily adsorb to hydrophilic solid supports so would be compatible with surface-based nanotechnologies, (iii) non-covalent systems allow greater flexibility to change the chromophore concen-

^aSchool of Physics and Astronomy, University of Leeds, Leeds LS2 9JT, UK.

E-mail: p.g.adams@leeds.ac.uk

^bAstbury Centre for Structural Molecular Biology, University of Leeds, Leeds LS2 9JT, UK

^cSchool of Biomedical Sciences, University of Leeds, Leeds LS2 9JT, UK

†Electronic supplementary information (ESI) available. See DOI: 10.1039/c9nr04653d



tration (or type), (iv) membranes allow the potential to co-assemble other components to make for a modular system (e.g. other photosynthetic proteins or any small amphiphiles).

Solution-based fluorescence spectroscopy is typically used to assess FRET in ensemble measurements. Fluorescence Lifetime Imaging Microscopy (FLIM) can improve upon this by measuring specific particles rather than the population average: it has been previously applied to map the fluorescence of LHCII proteins within nanoscale 2-D clusters,³⁰ micron-sized 3-D crystals³¹ and proteoliposomes,²⁵ quantifying its fluorescence quenching with ~ 300 nm resolution. Here, we present a new proof-of-concept system where LHCII is non-covalently interfaced with additional chromophores in the lipid membrane to enhance its spectral range over the 'green gap'. Samples are characterized with both ensemble spectroscopy and FLIM to provide a detailed quantitative assessment of their composition and FRET properties. Our results demonstrate the modularity, consistency and potential for highly efficient energy transfer of the non-covalent LHCII-chromophore systems.

Results and discussion

Concept and initial characterisation

LHCII protein was extracted from spinach leaves and biochemically purified using the detergent α -DDM, as previously described.³⁰ Denaturing and native gel electrophoresis indicate a high protein purity and the natural trimeric state (see Fig. S1 in the ESI[†]). We chose the small organic chromophore Texas Red (TR)³² as an ideal candidate for an energy donor to LHCII in membranes because of its complementary spectral properties and its amenability to assembly into lipid bilayers by tethering it to a lipid headgroup (TR-DHPE, as purchased).³³ Ensemble absorption and fluorescence spectroscopy was performed on isolated LHCII and TR to quantify their optical properties in an isolated state, as a baseline for comparison to the connected system. Our LHCII sample had the expected absorption spectrum with peaks representing chlorophyll (Chl) and carotenoids between 400–500 nm and the Q_y bands of Chl *b* and Chl *a* at 650 and 675 nm, respectively (Fig. 1A, green solid).³⁰ A single fluorescence emission peak at ~ 681.5 nm rep-

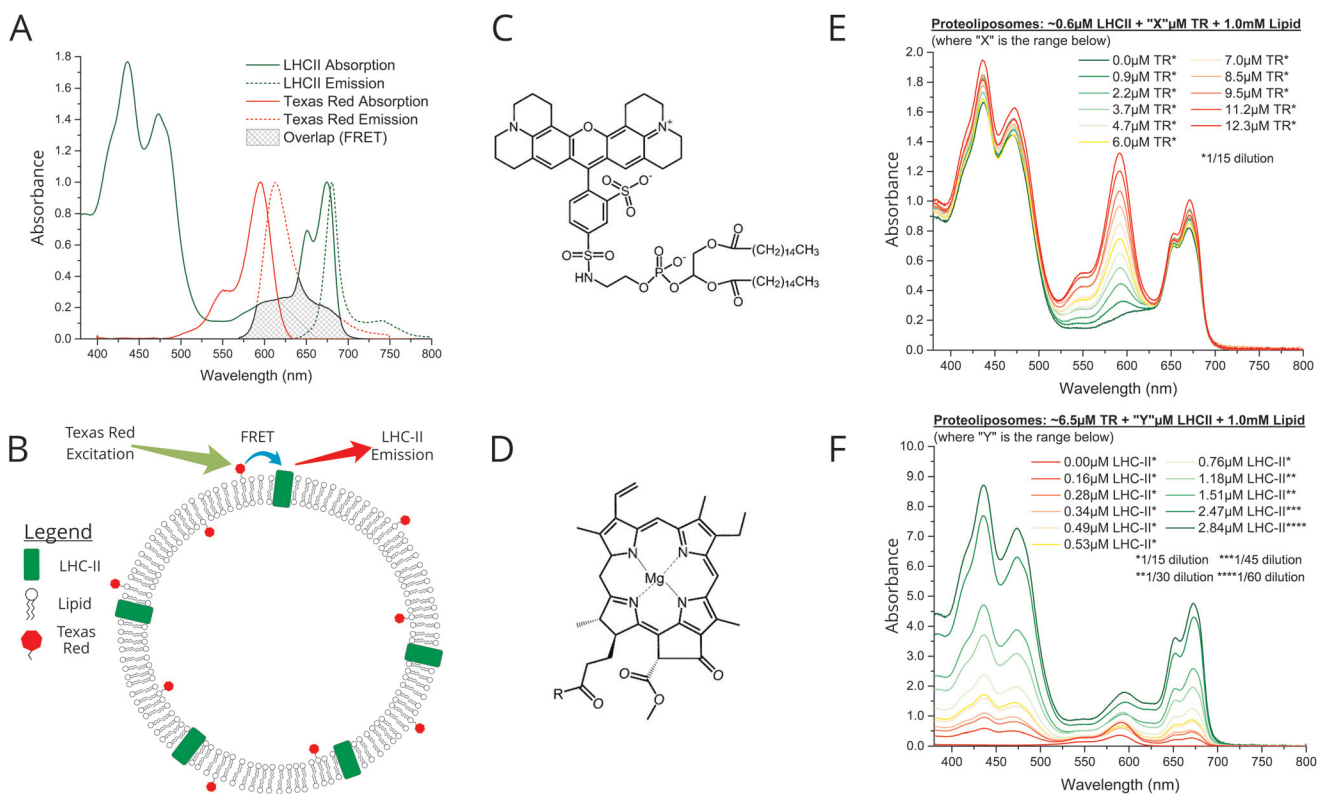


Fig. 1 (A) Ensemble solution-based spectroscopy performed on dilute samples of isolated LHCII or TR-DHPE in a detergent suspension: normalised absorption (solid line) and fluorescence emission (dotted line) spectra. These should be thought of as the starting material and compared with the assembled proteoliposomes. LHCII was excited at 473 nm, selective for Chl *b*, so that Chl *b* to Chl *a* energy transfer is monitored. TR was excited at 540 nm. Green: 0.4 nM LHCII trimers in a buffer of 0.03% w/v α -DDM, 10 mM HEPES, pH 7.5 (absorbance ~ 0.1 at 675 nm). Red: solution of liposomes comprised of 1.0 μ M TR-DHPE in a buffer of 0.1% w/v α -DDM, 10 mM HEPES, pH 7.5 (absorbance ~ 0.1 at 561 nm). The mean fluorescence lifetime of these samples were 3.9 ns and 4.4 ns, respectively (lifetime data shown in Fig. S6 in the ESI[†]). (B) Schematic concept of proteoliposomes with energy transfer direction and wavelengths indicated (not to scale). Chemical structures of (C) TR-DHPE (Texas Red 1,2-dihexadecanoyl-sn-glycero-3-phosphoethanolamine), and (D) chlorophyll *a*, where R = C₂₀H₄₀O (phytyl). Ensemble absorption spectra of (E) proteoliposome Series 1 and (F) proteoliposome Series 2. Samples were diluted prior to measurement and graphs are displayed after multiplication by these factors (annotated *).



resents emission from lowest energy Chl *a* indicating the highly-connected chlorophyll network that is expected within trimeric LHCII (Fig. 1A, green dotted).³⁰ The absorption of Texas Red is quite broad with a maximum at 591 nm (Fig. 1A, solid red), fitting well into the 'green gap' of LHCII. The TR fluorescence emission peak at 610 nm has extensive overlap with the LHCII Chl *b* absorption (Fig. 1A, dotted red), thus the excited state of TR is energetically close to chromophores within the intended acceptor LHCII. Therefore, high efficiency donor-to-acceptor FRET would be feasible if the chromophores can be arranged into close spatial proximity, as shown in the concept schematic Fig. 1B. The chemical structures of TR-DHPE and Chl *a* are shown in Fig. 1C and D for comparison.

We designed a procedure to co-reconstitute LHCII and TR-DHPE into membrane vesicles in a modular fashion, *i.e.*, for easy selection of the desired concentrations of each component. The protocol is similar to established proteoliposome formation procedures: initially both LHCII and lipids are solubilised in detergent (α -DDM), followed by gradual detergent removal using porous absorptive beads (Bio beads),^{26,28} causing the thermodynamically-driven self-assembly of membranes (see Materials and methods in ESI†). Analytical ultracentrifugation of proteoliposome *versus* control samples on density gradients suggested that the vesicles were a consistent and homogenous single population of diameter \sim 50–100 nm, with no evidence of any aggregated protein (see Fig. S2 in the ESI†). Some general observations can be made for all proteoliposome samples in comparison to isolated LHCII or TR-DHPE: (i) the TR absorption and fluorescence peaks do not shift, (ii) the LHCII absorption peaks have minimal shifts (<1 –3 nm), and (iii) the LHCII fluorescence peak is very similar (<1 nm shift, see Fig. S3 in the ESI†). Subtle spectral shifts of LHCII absorption could indicate slight changes in the local environment of chlorophylls (*e.g.*, protein conformation), however, good agreement of fluorescence excitation and linear absorption spectra suggest that the pigments within the protein are well connected (see Fig. S4 in ESI†). These results indicate that both TR-DHPE and LHCII are structurally and functionally intact within proteoliposomes.

Ensemble absorption and fluorescence spectroscopy

We wished to test whether a simple concept based on FRET could be applied to channel energy from Texas Red to LHCII in a controllable manner. From Förster theory one expects energy transfer efficiency (ETE) to depend on donor-acceptor distance *R*, *i.e.*, $ETE \propto 1/R^6$.^{34,35} Thus, one should be able to modulate energy transfer with the expectation of increasing ETE with increasing acceptor concentration and of increasing overall magnitude of transfer with increasing donor concentration.²² Samples were prepared in two series: aiming for either a constant acceptor content (Series 1) or a constant donor content (Series 2). The LHCII and TR-DHPE composition achieved in each proteoliposome sample was quantified *via* absorption spectroscopy and spectral decomposition analysis (see Fig. S5 in the ESI†). Incorporation yields of both

LHCII and TR were consistently high, between 75–85% and 80–90%, respectively (% of starting material successfully retained). As expected, Series 1 samples (Fig. 1E) had very similar LHCII concentrations of 0.52–0.61 μ M (8.6–9.4% of total proteoliposome mass) with a TR range from 0.9 to 12.3 μ M (0.09–1.2% of total lipid composition). Series 2 samples (Fig. 1F) had relatively similar TR concentrations of 5.0–8.4 μ M (0.5–0.84% of total lipid composition) with a LHCII range from 0.16 to 2.84 μ M (2.4–30.5% of total mass). Generation of this proteoliposome composition range demonstrates the modularity of our system with control over the incorporation of LHCII and TR-DHPE.

A well-defined system would be one where additional energy can be channelled to LHCII from extrinsic donors in a controllable manner. To estimate FRET efficiency the fluorescence of the donor chromophore in the combined system was compared to the donor-only system (*i.e.*, donor + acceptor *versus* isolated donors). Donor-to-acceptor energy transfer causes a quenching of the donor fluorescence, manifested as decreased intensity of its emission concomitant with a faster decay of its excited state, due to some excitons following this non-radiative pathway.²⁰ For our samples, the relative TR fluorescence intensity (TR emission per mole TR) was quantified in steady-state fluorescence emission spectra with selective excitation of TR. Proteoliposome Series 2 allowed analysis of how TR quenching depends upon LHCII concentration. A clear qualitative trend of decreasing TR fluorescence intensity with increasing LHCII concentration was observed, as an increasing amount of energy transfer occurs from TR to LHCII by FRET (Fig. 2A). Relative TR fluorescence quenched to as low as 2% of the control sample (isolated TR-DHPE) is found in proteoliposomes where LHCII concentration was at the maximum tested. Time-resolved fluorescence measurements were also performed as a secondary technique to independently quantify TR quenching, with selective excitation of TR. Fluorescence decay curves of proteoliposome Series 2 revealed a faster decay of TR fluorescence as LHCII concentration was increased (Fig. 2C), representing an increasing quenching, in correlation with the steady-state data. Fitting these curves to exponential decay functions reveal that the mean TR lifetime decreases from 4.4 ns in the absence of LHCII to a minimum of 0.7 ns at maximum LHCII concentration. As a further test, we took measurements before and after complete re-solubilisation of the membranes with excess α -DDM detergent. Re-solubilisation resulted in regeneration of highly fluorescent TR, confirming that its quenching is dependent on the membrane architecture allowing interaction with LHCII (see Fig. S7 in the ESI†).

Energy transfer from TR to LHCII was also apparent from observed increases in the relative LHCII fluorescence intensity (LHCII emission per mole LHCII) with selective excitation of TR. LHCII had only a low level of fluorescence without TR, but this increased significantly with increasing TR-DHPE concentration (Fig. 2B). The relative LHCII emission reached a maximum of 3.14 \times enhancement in the proteoliposomes with the highest TR-DHPE concentration, as compared to LHCII in proteoliposomes without TR.



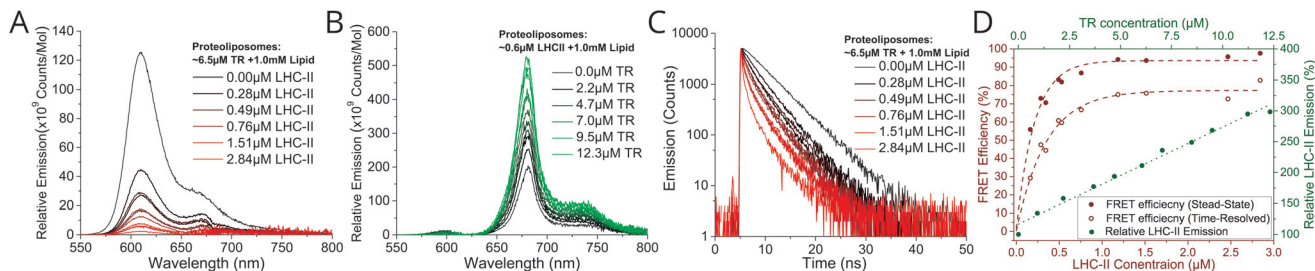


Fig. 2 (A) Relative fluorescence emission spectra of sample Series 2 with selective excitation of TR at 540 nm. (B) Relative fluorescence emission of sample Series 1 with selective excitation TR at 540 nm. For clarity, steady-state emission spectra were decomposed to subtract the non-relevant peak (see Fig S8 in ESI†). All spectra are displayed as the “relative emission” (*i.e.*, emission per mol of the relevant component). (C) Time-resolved fluorescence measurements of sample Series 2 with TR excitation by a 540 nm pulsed laser. Full dataset of fluorescence intensities and lifetimes are given in ESI Table S1.† (D) Red labelling, bottom and left axis: Energy Transfer Efficiency (ETE) versus LHCII concentration, calculated from proteoliposome Series 2, from both steady-state (ETE_{SS}) and time-resolved (ETE_{TR}) data using the conventional relationship for FRET between donor *D* and acceptor *A*: $[ETE]_{SS} = 1 - F_{DA}/F_D$ (1), where F_{DA} and F_D are the relative fluorescence intensity of TR in the presence or absence of LHCII, respectively, $[ETE]_{TR} = 1 - \tau_{DA}/\tau_D$ (2), where τ_{DA} and τ_D are the mean fluorescence lifetime of TR the presence or absence of LHCII, respectively. (D) Green labelling, top and right axis: relative LHCII emission versus TR concentration, calculated from proteoliposome Series 1. Note, the known phenomenon of self-quenching of LHCII fluorescence,^{24,25,28} was quantified in control samples omitting TR-DHPE (see Fig. S9 in the ESI†). Here, 100% is defined as the baseline intensity of LHCII emission observed for proteoliposomes containing 0.7 μM LHCII and 1 mM total lipid (as this is the average LHCII content for Series 1). Self-quenching of TR fluorescence was found to be minimal at 6.5 μM TR (see Fig. S10 in the ESI†).

Graphical analysis of fluorescence intensity and fluorescence lifetime data allowed the observed trends to be quantified. Energy transfer efficiency was calculated from both steady-state (ETE_{SS}) and time-resolved (ETE_{TR}) data, using standard equations (see figure legend). Fig. 2D (red datapoints) shows that efficiency increased non-linearly with LHCII concentration and is fitted to an exponential growth function, as efficiency is expected to saturate at high acceptor concentration. Steady-state and time-resolved data show good agreement of the trend and estimate a maximal ETE of $\sim 94\%$ and $\sim 77\%$, respectively (the exact value for ETE will be studied in future work, different spectroscopies often give different absolute values). This trend of ETE is attributed simply to the reduction in average distance between TR and LHCII as LHCII concentration is increased. The relative LHCII emission was found to increase in proportion to the concentration of TR-DHPE, for all concentrations investigated, see Fig. 2D green datapoints. This linear relationship is consistent with a constant TR-to-LHCII energy transfer efficiency irrespective of TR-DHPE concentration. Note that LHCII self-quenching and TR self-quenching was quantified in control samples and taken into account (see legend in Fig. 2). In summary, the proteoliposome system has well-defined donor-to-acceptor energy transfer and TR provides a controllable enhancement of LHCII emission demonstrating the benefit of increased spectral coverage in the ‘green gap’.

Functionality of LHCII-TR proteoliposomes on surfaces

Assessment of proteoliposome functionality when associated with planar surfaces is important for any future applications requiring thin films (*e.g.* in photo-active devices). Furthermore, microscopy is complementary to ensemble spectroscopy, allowing the identification and analysis of individual proteoliposomes. Fluorescence Lifetime Imaging Microscopy (FLIM)

was performed on two representative samples deposited onto glass coverslips in order to investigate population differences in samples with different energy transfer efficiencies: (i) “low-LHCII” proteoliposomes (1.2 μM LHCII + 6.5 μM TR-DHPE) and (ii) “high-LHCII” proteoliposomes (2.8 μM LHCII + 6.5 μM TR-DHPE). TR and LHCII were selectively excited with appropriate pulsed lasers and observed in dedicated detectors with appropriate emission filters (see Materials and methods in ESI†). This allowed visualisation of fluorescence intensity and fluorescent lifetimes for both TR and LHCII within individual proteoliposomes. Hundreds of well-resolved particles in each $25 \times 25 \mu\text{m}$ field of view were observed with apparent correlation in both TR and LHCII channel images (Fig. 3A). Quantitative analysis of these samples is non-trivial, and the effects of spectral overlap, photo-bleaching and detector noise were quantified and subtracted from all particles (see Materials and methods in ESI†). A population analysis of single proteoliposomes was undertaken by manually selecting particles within images, tabulating the data of fluorescence intensity and lifetimes, and performing statistics. These analyses allow the LHCII and TR to be independently identified in individual proteoliposomes revealing the extent of co-localisation the two fluorescent components. At least 83% and 80% of proteoliposomes had significant signal from both TR and LHCII emission channels, for low-LHCII and high-LHCII samples, respectively ($n = 200$, 99% confidence relative to background, see Table S2 in ESI†). This may underestimate the presence of LHCII, as smaller vesicles with little LHCII may not be detected. The vast majority of proteoliposomes in FLIM images appeared as diffraction-limited spots with measured widths of ~ 300 nm, suggesting that their true diameter is < 300 nm (see analysis in Fig S11 in the ESI†), in agreement with a likely diameter of ~ 100 nm measured from dynamic light scattering.



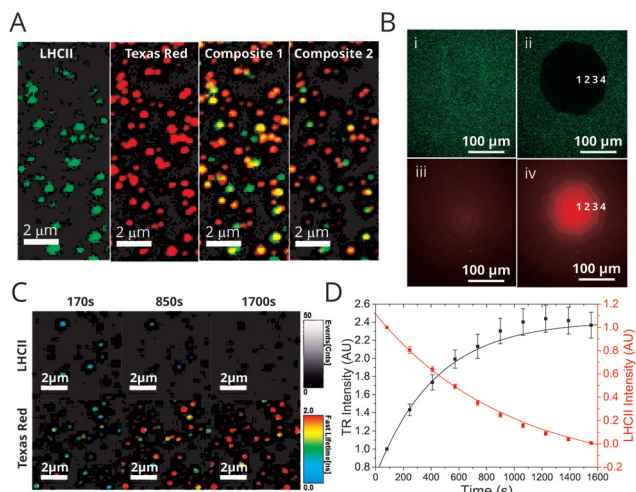


Fig. 3 Fluorescence microscopy and photo-bleaching data from proteoliposomes deposited on glass coverslips. See Materials and methods in ESI† for full details of sample preparation, image acquisition and analysis. (A) FLIM images of a representative field from a “high-LHCII” proteoliposome sample (2.8 μM LHCII, 6.5 μM TR, 1 mM total lipid) deposited at low surface density. Panels show the fluorescence intensity in either the LHCII channel, TR channel, or a Composite (both overlaid). Panels (i–iii) show a compressed intensity range (for clarity); panel (iv) shows a wider intensity range. Yellow colour in the composite image indicates strong co-localisation of signals from LHCII and TR. A gallery of images from other samples is shown in Fig. S12 in the ESI.† (B) Epifluorescence microscopy images of a representative proteoliposome sample (3.5 μM LHCII, 6.5 μM TR, 1 mM total lipid) deposited at high surface density. LHCII channel and TR channels were recorded sequentially using appropriate filter cubes. Bleaching was performed with high intensity of LHCII excitation through an aperture, the degree of photo-bleaching varied by iteratively opening the aperture in stages (numbered 1–4). (C) A time-lapse series of FLIM images of proteoliposomes, displaying both fluorescence intensity (brightness) and “fastFLIM lifetime” (colour scale). LHCII photo-bleaching occurs across the whole image, which decreases the quenching of TR. (D) Graph showing the total fluorescence intensity of the LHCII and TR channels versus time, for the sequence from (C).

Epifluorescence microscopy photo-bleaching experiments were performed to provide a visual representation of energy transfer, allowing us to assess whether optical functionality is retained when proteoliposomes are at high density on surfaces. LHCII was selectively photo-bleached in a confined region by exposing it to high intensity light through an appropriate filter and observing the effects in subsequent images. A very low LHCII fluorescence was observed in the bleach region (Fig. 3B, (i) vs. (ii)), whereas, the TR fluorescence in this region showed an apparent increase (Fig. 3B, (iii) vs. (iv)). This recovery of TR fluorescence (or “de-quenching”) confirms that photo-damaged LHCII is unable to act as an energy acceptor from Texas Red. FLIM was then used to analyse the photo-bleaching of proteoliposomes at lower surface densities and higher resolution. Bleaching occurs across the entire image region during continuous FLIM acquisition, but LHCII bleaches much faster than TR, allowing us to distinguish these effects. A decrease in LHCII fluorescence intensity with a concomitant increase in TR intensity is apparent in images of pro-

teoliposomes in Fig. 3C and is clear when plotting a time-course of the fluorescence intensity, Fig. 3D. The same trend apparent in epifluorescence data is visualized dynamically in the FLIM data, where the estimated TR lifetimes increase over time. ESI Video 1† shows this particularly clearly. By monitoring individual proteoliposomes across multiple images the fraction of proteoliposomes in which FRET occurs can be determined by the proxy of the TR recovery effect. Approximately 90% and 95% of proteoliposomes displayed a significant increase in TR lifetime, for low-LHCII and high-LHCII samples, respectively (significant defined as $\geq 125\%$ increase). The mean TR lifetime increased from 0.98 ± 0.54 ns to 2.75 ± 0.71 ns for ‘high-LHCII’ and from 1.15 ± 0.70 ns to 2.77 ± 0.76 ns for ‘low-LHCII’ ($n = 100$ for both). In summary, the photo-bleaching data from both epifluorescence and FLIM conclusively shows that the vast majority of proteoliposomes contain both LHCII and TR and that energy transfer between them is retained when these membranes are deposited onto a surface.

Analysis of single proteoliposomes by FLIM

In order to calculate the fluorescence lifetimes on a per-proteoliposome basis, manual analysis was performed by fitting fluorescence decay curves extracted from a region-of-interest defined to represent individual proteoliposomes. Decay curve fits from five representative proteoliposomes selected from a field in Fig. 4A are displayed in Fig. 4B, alongside calculated mean lifetimes of both TR and LHCII components. Frequency distributions of the TR lifetime for different proteoliposome samples (Fig. 4C) indicate that TR fluorescence is quenched by LHCII. The mean TR fluorescence lifetime decreases from 3.26 ± 0.46 ns in control TR liposomes (without LHCII) to 1.79 ± 0.64 ns and 1.46 ± 0.53 ns for “low-LHCII” and “high-LHCII” proteoliposomes, with a standard image acquisition time. Energy transfer efficiency (ETE) calculated after correction for photo-bleaching was plotted as a frequency distribution (Fig. 4D). We find a mean ETE \pm S.D. of $71 \pm 10\%$ and $77 \pm 8\%$ for “low-LHCII” and “high-LHCII” proteoliposomes, respectively. This shows that within a population, the ETE varies between individual proteoliposomes. It is interesting to note that a significant fraction of vesicles have an ETE $>90\%$ and we speculate that it may be possible to biochemically purify a sub-population of vesicles enriched for high ETE.^{23,40} In summary, the FLIM population distributions confirm that FRET occurs with increasing efficiency as LHCII concentration increases, in agreement with our ensemble spectroscopy data.

Future outlook: LH membranes as nanomaterials

We have significantly enhanced the effective absorption range of LHCII by using a proteoliposome-based system, *via* energy transfer from the spectrally complementary chromophore TR. Controlling the concentration of both LHCII and TR-DHPE as desired across an order of magnitude (Fig. 1) demonstrates the modularity of these membranes. Future studies could incorporate a suite of different organic chromophores and/or quantum dots into lipid bilayers to interact with LH proteins



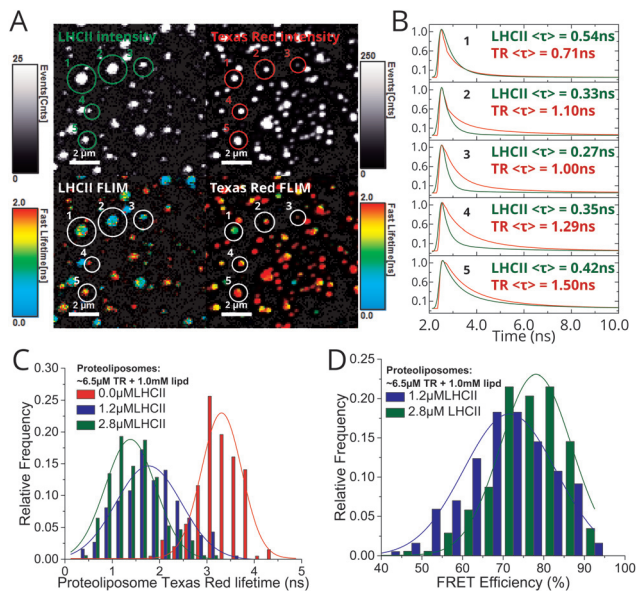


Fig. 4 FLIM data from proteoliposomes deposited at a low surface density on glass coverslips. See Materials and methods in ESI† for full details of the analyses. (A) Representative field from a high-LHCII proteoliposome sample (2.8 μM LHCII, 6.5 μM TR, 1 mM total lipid) imaged at high magnification, comparing fluorescence intensity (top) versus fluorescence lifetime (bottom) between LHCII and TR channels. Five representative particles have been indicated 1–5. (B) Fluorescence decay curve fits from the individual proteoliposomes, as numbered in (A), annotated with the calculated mean amplitude-weighted lifetimes (τ) of each component. Here, the fluorescence data from the 20–30 pixels representing one proteoliposome were binned, a decay curve generated, and fit to a biexponential decay function. (C) Frequency distribution histogram of the mean TR fluorescence lifetime, comparing the low-LHCII proteoliposome, high-LHCII proteoliposome and TR liposome samples ($n = 186, 175$ and 200 , respectively, see Table 2 in ESI†). Only well-resolved proteoliposomes with sufficient signal to produce a good fit were selected (counts >500 ; fitting $\chi^2 < 1.2$). The long acquisition provided sufficient counts for good fits, but caused photo-bleaching of LHCII resulting in a distortion of the TR lifetime towards larger values. (D) Frequency distribution histogram of the ETE comparing the low-LHCII vs. high-LHCII proteoliposomes, calculated as in Fig. 2 eqn (2) using the data from (C). A correction factor determined from control samples is applied to account for TR lifetime distortion (see Table 3 in ESI†).

to enhance their spectral range further. Our group previously demonstrated diblock copolymer assemblies can also be used as a matrix to arrange organic chromophores for high efficiency FRET^{20–22} and may be more robust than lipids, but polymers are not a natural environment for proteins. We speculate that a polymer-lipid hybrid^{37,38} system could be tuned to combine the advantages of a more robust polymeric system and the protein compatibility of lipids.

Energy transfer between TR and LHCII in proteoliposomes was highly efficient (Fig. 2), comparable to systems utilising covalent attachment of chromophores to the protein,^{11–14} and is consistent with theoretical modelling of a system that has a random distribution of chromophores throughout a 2D lipid bilayer undergoing simple donor-to-acceptor FRET.³⁹ By exploiting the self-assembly of lipids and membrane proteins

into nano-sized architectures the distance between TR and LHCII is shortened, whereas, when not confined to these nanoscale membranes (*e.g.* when solubilised by detergent) the energy transfer drops to almost zero. This, together with our single-proteoliposome FLIM data, suggests that our self-assembly protocol creates a well-mixed environment on the nanoscale, addressing the challenge of inconsistent distribution of membrane proteins between proteoliposomes that was previously reported with other similar methods,²³ with the possibility that further purification could isolate sub-populations with desirable properties.⁴⁰ Proteoliposomes have potential to improve our understanding of the photophysical properties of LH proteins, for example, the transient interactions between diffusing chromophores and LH proteins could be assessed using ultrafast spectroscopy.^{13,36}

Our LHCII/TR proteoliposomes were found to retain their energy transfer efficiency when deposited onto solid supports (Fig. 3), providing proof-of-principle that they would be amenable to surface-based applications. Previous studies have shown that LH proteins attached to glass surfaces in nanoscale array patterns provide directional transfer of energy^{41,42} and that the absorption efficiencies of LH proteins can be enhanced by exploiting plasmon resonances of metal surfaces, *e.g.*, silver nanowires.⁴³ Expanding these ideas to make use of LHCII/TR proteoliposomes, future studies could pattern lipid bilayers incorporating any LH proteins and additional chromophores desired³³ to generate surface-supported organized nanoscale membranes which have enhanced light-harvesting capability.

Importantly, our single-particle FLIM analyses prove that our proteoliposomes are have quantitatively similar FRET on surfaces as in solution in bulk (Fig. 4). Our study is one of the few where single-molecule spectroscopy was utilised to quantify distributions of fluorescence lifetime in membrane reconstituted light-harvesting systems²⁵ beyond traditional ensemble spectroscopy. Observing the heterogeneity in this way could reveal low-frequency events and also guide the optimization of the system if one wishes to maximize any aspect, *e.g.* transfer efficiency. With developments in depositing thylakoid lipid thin films on surfaces,⁴⁴ our system has future potential applications as a photo-active bio-hybrid material, for example as coatings to enhance the current generated by photoelectrochemical devices.^{45,46}

Experimental section

A full experimental section describing the materials, methods and analysis is given in the ESI.† All relevant raw and analysed data associated with this paper are openly available under a CC-BY license in the Research Data Leeds repository⁴⁷ under DOI: 10.5518/611.

Conflicts of interest

There are no conflicts of interest to declare.



Acknowledgements

A. M. H. was supported by an Engineering and Physical Sciences Research Council (EPSRC, UK) studentship, award number 1807029, and an EPSRC programme grant, EP/J017566/1 "CAPITALs". S. A. M. was supported by a Biotechnology and Biological Sciences Research Council (BBSRC, UK) studentship, award number 1940236. S. D. C. was also supported by EPSRC "CAPITALs" award EP/J017566/1. L. J. C. J. is grateful to the BBSRC for funding (BB/P005454/1). P. G. A. was supported by a Future Leader Fellowship from the BBSRC, award number BB/M013723/1, and a University Academic Fellowship (University of Leeds). The PicoQuant FLIM instrument was acquired at Leeds with funding from a BBSRC award number BB/R000174/1, and the Quantamaster fluorescence spectrometer was funded by BBSRC award number BB/R000271/1.

P. G. A. thanks Eliot Dawson (Leeds) for the preliminary work he performed on this project.

References

- 1 D. Gust, T. A. Moore and A. L. Moore, Solar Fuels via Artificial Photosynthesis, *Acc. Chem. Res.*, 2009, **42**(12), 1890–1898.
- 2 X. M. Li, S. P. Qiao, L. L. Zhao, S. D. Liu, F. Li, F. H. Yang, Q. Luo, C. X. Hou, J. Y. Xu and J. Q. Liu, Template-Free Construction of Highly Ordered Monolayered Fluorescent Protein Nanosheets: A Bioinspired Artificial Light-Harvesting System, *ACS Nano*, 2019, **13**(2), 1861–1869.
- 3 S. Berhanu, T. Ueda and Y. Kuruma, Artificial photosynthetic cell producing energy for protein synthesis, *Nat. Commun.*, 2019, **10**, 1325.
- 4 C. Liu, J. J. Gallagher, K. K. Sakimoto, E. M. Nichols, C. J. Chang, M. C. Y. Chang and P. D. Yang, Nanowire-Bacteria Hybrids for Unassisted Solar Carbon Dioxide Fixation to Value-Added Chemicals, *Nano Lett.*, 2015, **15**(5), 3634–3639.
- 5 J. Qiu, G. T. Zeng, M. A. Ha, M. Y. Ge, Y. J. Lin, M. Hettick, B. Y. Hou, A. N. Alexandrova, A. Javey and S. B. Cronin, Artificial Photosynthesis on TiO₂-Passivated InP Nanopillars, *Nano Lett.*, 2015, **15**(9), 6177–6181.
- 6 H. C. Sun, X. Y. Zhang, L. Miao, L. L. Zhao, Q. Luo, J. Y. Xu and J. Q. Liu, Micelle-Induced Self-Assembling Protein Nanowires: Versatile Supramolecular Scaffolds for Designing the Light-Harvesting System, *ACS Nano*, 2016, **10**(1), 421–428.
- 7 R. E. Blankenship, D. M. Tiede, J. Barber, G. W. Brudvig, G. Fleming, M. Ghirardi, M. R. Gunner, W. Junge, D. M. Kramer, A. Melis, T. A. Moore, C. C. Moser, D. G. Nocera, A. J. Nozik, D. R. Ort, W. W. Parson, R. C. Prince and R. T. Sayre, Comparing Photosynthetic and Photovoltaic Efficiencies and Recognizing the Potential for Improvement, *Science*, 2011, **332**(6031), 805–809.
- 8 J. L. Gao, H. Wang, Q. P. Yuan and Y. Feng, Structure and Function of the Photosystem Supercomplexes, *Front. Plant Sci.*, 2018, **9**, 357.
- 9 T. Mirkovic, E. E. Ostroumov, J. M. Anna, R. van Grondelle, Govindjee and G. D. Scholes, Light Absorption and Energy Transfer in the Antenna Complexes of Photosynthetic Organisms, *Chem. Rev.*, 2017, **117**(2), 249–293.
- 10 J. Standfuss, A. C. T. van Scheltinga, M. Lamborghini and W. Kuhlbrandt, Mechanisms of photoprotection and non-photochemical quenching in pea light-harvesting complex at 2.5 Å resolution, *EMBO J.*, 2005, **24**(5), 919–928.
- 11 K. Gundlach, M. Werwie, S. Wiegand and H. Paulsen, Filling the "green gap" of the major light-harvesting chlorophyll a/b complex by covalent attachment of Rhodamine Red, *Biochim. Biophys. Acta, Bioenerg.*, 2009, **1787**(12), 1499–1504.
- 12 M. A. Harris, J. Jiang, D. M. Niedzwiedzki, J. Jiao, M. Taniguchi, C. Kirmaier, P. A. Loach, D. F. Bocian, J. S. Lindsey, D. Holten and P. S. Parkes-Loach, Versatile design of biohybrid light-harvesting architectures to tune location, density, and spectral coverage of attached synthetic chromophores for enhanced energy capture, *Photosynth. Res.*, 2014, **121**(1), 35–48.
- 13 Y. Yoneda, T. Noji, T. Katayama, N. Mizutani, D. Komori, M. Nango, H. Miyasaka, S. Itoh, Y. Nagasawa and T. Dewa, Extension of Light-Harvesting Ability of Photosynthetic Light-Harvesting Complex 2 (LH2) through Ultrafast Energy Transfer from Covalently Attached Artificial Chromophores, *J. Am. Chem. Soc.*, 2015, **137**(40), 13121–13129.
- 14 J. W. Springer, P. S. Parkes-Loach, K. R. Reddy, M. Krayner, J. Jiao, G. M. Lee, D. M. Niedzwiedzki, M. A. Harris, C. Kirmaier, D. F. Bocian, J. S. Lindsey, D. Holten and P. A. Loach, Biohybrid Photosynthetic Antenna Complexes for Enhanced Light-Harvesting, *J. Am. Chem. Soc.*, 2012, **134**(10), 4589–4599.
- 15 F. J. Schmitt, E. G. Maksimov, P. Hätti, J. Weissenborn, V. Jeyasangar, A. P. Razjivin, V. Z. Paschenko, T. Friedrich and G. Renger, Coupling of different isolated photosynthetic light harvesting complexes and CdSe/ZnS nanocrystals via Förster resonance energy transfer, *Biochim. Biophys. Acta, Bioenerg.*, 2012, **1817**(8), 1461–1470.
- 16 M. Werwie, X. Xu, M. Haase, T. Basche and H. Paulsen, Bio Serves Nano: Biological Light-Harvesting Complex as Energy Donor for Semiconductor Quantum Dots, *Langmuir*, 2012, **28**(13), 5810–5818.
- 17 T. Sahin, M. A. Harris, P. Vairaprakash, D. M. Niedzwiedzki, V. Subramanian, A. P. Shreve, D. F. Bocian, D. Holten and J. S. Lindsey, Self-Assembled Light-Harvesting System from Chromophores in Lipid Vesicles, *J. Phys. Chem. B*, 2015, **119**(32), 10231–10243.
- 18 V. De Leo, L. Catucci, A. Falqui, R. Marotta, M. Striccoli, A. Agostiano, R. Comparelli and F. Milano, Hybrid Assemblies of Fluorescent Nanocrystals and Membrane Proteins in Liposomes, *Langmuir*, 2014, **30**(6), 1599–1608.
- 19 E. P. Lukashev, P. P. Knox, V. V. Gorokhov, N. P. Grishanova, N. K. Seifullina, M. Krikunova, H. Lokstein and V. Z. Paschenko, Purple-bacterial photosynthetic reaction centers and quantum-dot hybrid-assembly



- blies in lecithin liposomes and thin films, *J. Photochem. Photobiol., B*, 2016, **164**(Supplement C), 73–82.
- 20 P. G. Adams, A. M. Collins, T. Sahin, V. Subramanian, V. S. Urban, P. Vairaprakash, Y. Tian, D. G. Evans, A. P. Shreve and G. A. Montano, Diblock copolymer micelles and supported films with noncovalently incorporated chromophores: a modular platform for efficient energy transfer, *Nano Lett.*, 2015, **15**(4), 2422–2428.
 - 21 G. S. Orf, A. M. Collins, D. M. Niedzwiedzki, M. Tank, V. Thiel, A. Kell, D. A. Bryant, G. A. Montano and R. E. Blankenship, Polymer-Chlorosome Nanocomposites Consisting of Non-Native Combinations of Self-Assembling Bacteriochlorophylls, *Langmuir*, 2017, **33**(25), 6427–6438.
 - 22 A. M. Collins, J. A. Timlin, S. M. Anthony and G. A. Montano, Amphiphilic block copolymers as flexible membrane materials generating structural and functional mimics of green bacterial antenna complexes, *Nanoscale*, 2016, **8**(32), 15056–15063.
 - 23 M. Tutkus, P. Akhtar, J. Chmeliov, F. Gorföl, G. Trinkunas, P. H. Lambrev and L. Valkunas, Fluorescence Microscopy of Single Liposomes with Incorporated Pigment-Proteins, *Langmuir*, 2018, **34**(47), 14410–14418.
 - 24 I. Moya, M. Silvestri, O. Vallon, G. Cinque and R. Bassi, Time-Resolved Fluorescence Analysis of the Photosystem II Antenna Proteins in Detergent Micelles and Liposomes, *Biochemistry*, 2001, **40**, 12552–12561.
 - 25 A. Natali, J. M. Gruber, L. Dietzel, M. C. Stuart, R. van Grondelle and R. Croce, Light-harvesting Complexes (LHCs) Cluster Spontaneously in Membrane Environment Leading to Shortening of Their Excited State Lifetimes, *J. Biol. Chem.*, 2016, **291**(32), 16730–16739.
 - 26 D. Seiwert, H. Witt, S. Ritz, A. Janshoff and H. Paulsen, The Nonbilayer Lipid MGDG and the Major Light-Harvesting Complex (LHCII) Promote Membrane Stacking in Supported Lipid Bilayers, *Biochemistry*, 2018, **57**(15), 2278–2288.
 - 27 F. Zhou, S. Liu, Z. Hu, T. Kuang, H. Paulsen and C. Yang, Effect of monogalactosyldiacylglycerol on the interaction between photosystem II core complex and its antenna complexes in liposomes of thylakoid lipids, *Photosynth. Res.*, 2009, **99**(3), 185–193.
 - 28 E. Crisafi and A. Pandit, Disentangling protein and lipid interactions that control a molecular switch in photosynthetic light harvesting, *Biochim. Biophys. Acta, Biomembr.*, 2017, **1859**(1), 40–47.
 - 29 A. Pandit, N. Shirzad-Wasei, L. M. Wlodarczyk, H. van Roon, E. J. Boekema, J. P. Dekker and W. J. de Grip, Assembly of the major light-harvesting complex II in lipid nanodiscs, *Biophys. J.*, 2011, **101**(10), 2507–2515.
 - 30 P. G. Adams, C. Vasilev, C. N. Hunter and M. P. Johnson, Correlated fluorescence quenching and topographic mapping of Light-Harvesting Complex II within surface-assembled aggregates and lipid bilayers, *Biochim. Biophys. Acta, Bioenerg.*, 2018, **1859**(10), 1075–1085.
 - 31 B. van Oort, A. Marechal, A. V. Ruban, B. Robert, A. A. Pascal, N. C. de Ruijter, R. van Grondelle and H. van Amerongen, Different crystal morphologies lead to slightly different conformations of light-harvesting complex II as monitored by variations of the intrinsic fluorescence lifetime, *Phys. Chem. Chem. Phys.*, 2011, **13**(27), 12614–12622.
 - 32 J. A. Titus, R. Haugland, S. O. Sharrow and D. M. Segal, Texas red, a hydrophilic, red-emitting fluorophore for use with fluorescein in dual parameter flow microfluorometric and fluorescence microscopic studies, *J. Immunol. Methods*, 1982, **50**(2), 193–204.
 - 33 P. G. Adams, K. L. Swingle, W. F. Paxton, J. J. Nogan, L. R. Stromberg, M. A. Firestone, H. Mukundan and G. A. Montano, Exploiting lipopolysaccharide-induced deformation of lipid bilayers to modify membrane composition and generate two-dimensional geometric membrane array patterns, *Sci. Rep.*, 2015, **5**, 10331.
 - 34 T. Förster, Delocalized excitation and excitation transfer, *Modern Quantum Chemistry Istanbul Lectures*, 1965, vol. 3, pp. 93–137.
 - 35 K. F. Fox, V. Balevicius, J. Chmeliov, L. Valkunas, A. V. Ruban and C. D. P. Duffy, The carotenoid pathway: what is important for excitation quenching in plant antenna complexes?, *Phys. Chem. Chem. Phys.*, 2017, **19**(34), 22957–22968.
 - 36 J. I. Ogren, A. L. Tong, S. C. Gordon, A. Chenu, Y. Lu, R. E. Blankenship, J. Cao and G. S. Schlau-Cohen, Impact of the lipid bilayer on energy transfer kinetics in the photosynthetic protein LH2, *Chem. Sci.*, 2018, **9**(12), 3095–3104.
 - 37 R. Seneviratne, S. Khan, E. Moscrop, M. Rappolt, S. P. Muench, L. J. C. Jeuken and P. A. Beales, A reconstitution method for integral membrane proteins in hybrid lipid-polymer vesicles for enhanced functional durability, *Methods*, 2018, **147**, 142–149.
 - 38 L. Otrin, N. Marusic, C. Bednarz, T. Vidakovic-Koch, I. Lieberwirth, K. Landfester and K. Sundmacher, Toward Artificial Mitochondrion: Mimicking Oxidative Phosphorylation in Polymer and Hybrid Membranes, *Nano Lett.*, 2017, **17**(11), 6816–6821.
 - 39 V. Subramanian, N. A. Zurek, D. G. Evans and A. P. Shreve, Predictive modeling of broad wavelength light-harvesting performance in assemblies of multiple chromophores, *J. Photochem. Photobiol., A*, 2018, **367**, 105–114.
 - 40 P. Akhtar, F. Gorföl, G. Garab and P. H. Lambrev, Dependence of chlorophyll fluorescence quenching on the lipid-to-protein ratio in reconstituted light-harvesting complex II membranes containing lipid labels, *Chem. Phys.*, 2019, **522**, 242–248.
 - 41 C. Vasilev, M. P. Johnson, E. Gonzales, L. Wang, A. V. Ruban, G. Montano, A. J. Cadby and C. N. Hunter, Reversible Switching between Nonquenched and Quenched States in Nanoscale Linear Arrays of Plant Light-Harvesting Antenna Complexes, *Langmuir*, 2014, **30**(28), 8481–8490.
 - 42 M. Escalante, A. Lenferink, Y. Zhao, N. Tas, J. Huskens, C. N. Hunter, V. Subramanian and C. Otto, Long-Range Energy Propagation in Nanometer Arrays of Light Harvesting Antenna Complexes, *Nano Lett.*, 2010, **10**(4), 1450–1457.



- 43 M. Szalkowski, J. D. Janna Olmos, D. Buczynska, S. Mackowski, D. Kowalska and J. Kargul, Plasmon-induced absorption of blind chlorophylls in photosynthetic proteins assembled on silver nanowires, *Nanoscale*, 2017, **9**(29), 10475–10486.
- 44 O. Grab, M. Abacilar, F. Daus, A. Geyer and C. Steinem, 3D-Membrane Stacks on Supported Membranes Composed of Diatom Lipids Induced by Long-Chain Polyamines, *Langmuir*, 2016, **32**(39), 10144–10152.
- 45 P. N. Ciesielski, C. J. Faulkner, M. T. Irwin, J. M. Gregory, N. H. Tolk, D. E. Cliffel and G. K. Jennings, Enhanced Photocurrent Production by Photosystem I Multilayer Assemblies, *Adv. Funct. Mater.*, 2010, **20**(23), 4048–4054.
- 46 S. K. Ravi, Z. M. Yu, D. J. K. Swainsbury, J. Y. Ouyang, M. R. Jones and S. C. Tan, Enhanced Output from Biohybrid Photoelectrochemical Transparent Tandem Cells Integrating Photosynthetic Proteins Genetically Modified for Expanded Solar Energy Harvesting, *Adv. Energy Mater.*, 2017, **7**(7), 601821.
- 47 A. M. Hancock, S. A. Meredith, S. D. Connell, L. J. C. Jeuken and P. G. Adams, *Dataset for the study of proteoliposomes as energy-transferring materials: enhancing the spectral range of light-harvesting proteins using lipid-linked chromophores*, University of Leeds, 2019, [Dataset]: DOI: 10.5518/611.

